

Discrete plasmonic solitons in graphene-coated nanowire arrays

Yao Kou* and Jens Förstner

Department of Electrical Engineering, Paderborn University, Warburger Str. 100, 33098 Paderborn, Germany
yao.kou@uni-paderborn.de

Abstract: We study the discrete soliton formation in one- and two-dimensional arrays of nanowires coated with graphene monolayers. Highly confined solitons, including the fundamental and the higher-order modes, are found to be supported by the proposed structure with a low level of power flow. Numerical analysis reveals that, by tuning the input intensity and Fermi energy, the beam diffraction, soliton dimension and propagation loss can be fully controlled in a broad range, indicating potential values of the graphene-based solitons in nonlinear/active nanophotonic systems.

©2016 Optical Society of America

OCIS codes: (190.4390) Nonlinear optics, integrated optics; (250.5403) Plasmonics; (190.6135) Spatial solitons.

References and links

1. M. Kauranen and A. V. Zayats, "Nonlinear plasmonics," *Nat. Photonics* **6**(11), 737–748 (2012).
2. F. Ye, D. Mihalache, B. Hu, and N. C. Panoiu, "Subwavelength plasmonic lattice solitons in arrays of metallic nanowires," *Phys. Rev. Lett.* **104**(10), 106802 (2010).
3. Y. Liu, G. Bartal, D. A. Genov, and X. Zhang, "Subwavelength discrete solitons in nonlinear metamaterials," *Phys. Rev. Lett.* **99**(15), 153901 (2007).
4. A. R. Davoyan, I. V. Shadrivov, and Y. S. Kivshar, "Self-focusing and spatial plasmon-polariton solitons," *Opt. Express* **17**(24), 21732–21737 (2009).
5. M. Jablan, H. Buljan, and M. Soljačić, "Plasmonics in graphene at infrared frequencies," *Phys. Rev. B* **80**(24), 245435 (2009).
6. F. Bonaccorso, Z. Sun, T. Hasan, and A. Ferrari, "Graphene photonics and optoelectronics," *Nat. Photonics* **4**(9), 611–622 (2010).
7. F. H. Koppens, D. E. Chang, and F. J. García de Abajo, "Graphene plasmonics: a platform for strong light-matter interactions," *Nano Lett.* **11**(8), 3370–3377 (2011).
8. A. K. Geim, "Graphene: status and prospects," *Science* **324**(5934), 1530–1534 (2009).
9. K. Kim, J.-Y. Choi, T. Kim, S.-H. Cho, and H.-J. Chung, "A role for graphene in silicon-based semiconductor devices," *Nature* **479**(7373), 338–344 (2011).
10. J. Gosciniaik and D. T. Tan, "Graphene-based waveguide integrated dielectric-loaded plasmonic electro-absorption modulators," *Nanotechnology* **24**(18), 185202 (2013).
11. A. V. Gorbach, A. Marini, and D. V. Skryabin, "Graphene-clad tapered fiber: effective nonlinearity and propagation losses," *Opt. Lett.* **38**(24), 5244–5247 (2013).
12. X. Yang, K. Fan, Y. Zhu, J. Shen, X. Jiang, P. Zhao, S. Luan, and C. Li, "Electric papers of graphene-coated Co_3O_4 fibers for high-performance lithium-ion batteries," *ACS Appl. Mater. Interfaces* **5**(3), 997–1002 (2013).
13. Y. Wu, B. Yao, A. Zhang, Y. Rao, Z. Wang, Y. Cheng, Y. Gong, W. Zhang, Y. Chen, and K. S. Chiang, "Graphene-coated microfiber Bragg grating for high-sensitivity gas sensing," *Opt. Lett.* **39**(5), 1235–1237 (2014).
14. Y. Gao, G. Ren, B. Zhu, J. Wang, and S. Jian, "Single-mode graphene-coated nanowire plasmonic waveguide," *Opt. Lett.* **39**(20), 5909–5912 (2014).
15. Y. Gao, G. Ren, B. Zhu, H. Liu, Y. Lian, and S. Jian, "Analytical model for plasmon modes in graphene-coated nanowire," *Opt. Express* **22**(20), 24322–24331 (2014).
16. H. Wang, Y. Yang, Y. Liang, J. T. Robinson, Y. Li, A. Jackson, Y. Cui, and H. Dai, "Graphene-wrapped sulfur particles as a rechargeable lithium-sulfur battery cathode material with high capacity and cycling stability," *Nano Lett.* **11**(7), 2644–2647 (2011).
17. D. A. Smirnova, I. V. Shadrivov, A. E. Miroschnichenko, A. I. Smirnov, and Y. S. Kivshar, "Second-harmonic generation by a graphene nanoparticle," *Phys. Rev. B* **90**(3), 035412 (2014).
18. R. Alaei, M. Farhat, C. Rockstuhl, and F. Lederer, "A perfect absorber made of a graphene micro-ribbon metamaterial," *Opt. Express* **20**(27), 28017–28024 (2012).
19. A. Y. Nikitin, F. Guinea, F. Garcia-Vidal, and L. Martin-Moreno, "Surface plasmon enhanced absorption and suppressed transmission in periodic arrays of graphene ribbons," *Phys. Rev. B* **85**(8), 081405 (2012).
20. M. A. Othman, C. Guclu, and F. Capolino, "Graphene-based tunable hyperbolic metamaterials and enhanced near-field absorption," *Opt. Express* **21**(6), 7614–7632 (2013).

21. T. Low and P. Avouris, "Graphene plasmonics for terahertz to mid-infrared applications," *ACS Nano* **8**(2), 1086–1101 (2014).
22. J. Christensen, A. Manjavacas, S. Thongrattanasiri, F. H. L. Koppens, and F. J. García de Abajo, "Graphene plasmon waveguiding and hybridization in individual and paired nanoribbons," *ACS Nano* **6**(1), 431–440 (2012).
23. K. F. Mak, M. Y. Sfeir, Y. Wu, C. H. Lui, J. A. Misewich, and T. F. Heinz, "Measurement of the optical conductivity of graphene," *Phys. Rev. Lett.* **101**(19), 196405 (2008).
24. W. Gao, J. Shu, C. Qiu, and Q. Xu, "Excitation of plasmonic waves in graphene by guided-mode resonances," *ACS Nano* **6**(9), 7806–7813 (2012).
25. P. Avouris, "Graphene: electronic and photonic properties and devices," *Nano Lett.* **10**(11), 4285–4294 (2010).
26. Q. Bao and K. P. Loh, "Graphene photonics, plasmonics, and broadband optoelectronic devices," *ACS Nano* **6**(5), 3677–3694 (2012).
27. E. Hendry, P. J. Hale, J. Moger, A. K. Savchenko, and S. A. Mikhailov, "Coherent nonlinear optical response of graphene," *Phys. Rev. Lett.* **105**(9), 097401 (2010).
28. S.-Y. Hong, J. I. Dadap, N. Petrone, P.-C. Yeh, J. Hone, and R. M. Osgood, Jr., "Optical third-harmonic generation in graphene," *Phys. Rev. X* **3**(2), 021014 (2013).
29. D. A. Smirnova, A. V. Gorbach, I. V. Iorsh, I. V. Shadrivov, and Y. S. Kivshar, "Nonlinear switching with a graphene coupler," *Phys. Rev. B* **88**(4), 045443 (2013).
30. M. I. Molina and Y. S. Kivshar, "Discrete and surface solitons in photonic graphene nanoribbons," *Opt. Lett.* **35**(17), 2895–2897 (2010).
31. Y. V. Bludov, D. A. Smirnova, Y. S. Kivshar, N. M. Peres, and M. I. Vasilevskiy, "Discrete solitons in graphene metamaterials," *Phys. Rev. B* **91**(4), 045424 (2015).
32. D. A. Smirnova, R. E. Noskov, L. A. Smirnov, and Y. S. Kivshar, "Dissipative plasmon solitons in graphene nanodisk arrays," *Phys. Rev. B* **91**(7), 075409 (2015).
33. D. A. Smirnova, I. V. Shadrivov, A. I. Smirnov, and Y. S. Kivshar, "Dissipative plasmon-solitons in multilayer graphene," *Laser Photonics Rev.* **8**(2), 291–296 (2014).
34. C. Huang, F. Ye, Z. Sun, and X. Chen, "Tunable subwavelength photonic lattices and solitons in periodically patterned graphene monolayer," *Opt. Express* **22**(24), 30108–30117 (2014).
35. A. Savin and Y. S. Kivshar, "Surface solitons at the edges of graphene nanoribbons," *Europhysics Lett.* **89**(4), 46001 (2010).
36. M. L. Nesterov, J. Bravo-Abad, A. Y. Nikitin, F. J. García-Vidal, and L. Martín-Moreno, "Graphene supports the propagation of subwavelength optical solitons," *Laser Photonics Rev.* **7**(2), L7–L11 (2013).
37. L. M. Zhao, D. Y. Tang, H. Zhang, X. Wu, Q. Bao, and K. P. Loh, "Dissipative soliton operation of an ytterbium-doped fiber laser mode locked with atomic multilayer graphene," *Opt. Lett.* **35**(21), 3622–3624 (2010).
38. S. Mikhailov, "Non-linear electromagnetic response of graphene," *Europhysics Lett.* **79**(2), 27002 (2007).
39. R. Wang, Y. Hao, Z. Wang, H. Gong, and J. T. L. Thong, "Large-diameter graphene nanotubes synthesized using Ni nanowire templates," *Nano Lett.* **10**(12), 4844–4850 (2010).
40. Y. Wu, B. Yao, A. Zhang, Y. Rao, Z. Wang, Y. Cheng, Y. Gong, W. Zhang, Y. Chen, and K. S. Chiang, "Graphene-coated microfiber Bragg grating for high-sensitivity gas sensing," *Opt. Lett.* **39**(5), 1235–1237 (2014).
41. A. Roberts, D. Cormode, C. Reynolds, T. Newhouse-Illige, B. J. LeRoy, and A. S. Sandhu, "Response of graphene to femtosecond high-intensity laser irradiation," *Appl. Phys. Lett.* **99**(5), 051912 (2011).
42. I. Khrapach, F. Withers, T. H. Bointon, D. K. Polyushkin, W. L. Barnes, S. Russo, and M. F. Craciun, "Novel highly conductive and transparent graphene-based conductors," *Adv. Mater.* **24**(21), 2844–2849 (2012).
43. K. I. Bolotin, K. J. Sikes, Z. Jiang, M. Klima, G. Fudenberg, J. Hone, P. Kim, and H. L. Stormer, "Ultrahigh electron mobility in suspended graphene," *Solid State Commun.* **146**(9–10), 351–355 (2008).
44. P. Neugebauer, M. Orlita, C. Faugeras, A.-L. Barra, and M. Potemski, "How perfect can graphene be?" *Phys. Rev. Lett.* **103**(13), 136403 (2009).

1. Introduction

The nonlinear (NL) optics in plasmonic nano-structures has recently become a very attractive area of scientific research, owing to its important role in nanoscale signal processing, where light flows are expected to be restricted, guided, and manipulated efficiently in a small volume [1]. On the metal surfaces, electromagnetic waves are intensively enhanced, thus enable strong nonlinear effects to be manifested under a short spatial scale with relatively low power. A concrete example is the generation of plasmonic solitons in the metal-NL dielectric composites [2–4], where the self-actions of subwavelength localized beams were demonstrated.

Compared with noble metals, graphene, the two-dimensional atomic-thickness carbon sheet, opens novel opportunities for the surface plasmon operations in a wide frequency range from THz to infrared, with striking optical and electronic properties [5–7]. When utilized in photonic integration, the graphene layer benefits from its excellent mechanical robustness and pliability [8], making the material feasible to be tailored, wrapped, or assembled with other

dielectric/metal structures, such as ridges [9, 10], fibers [11–13], nanowires [14, 15] and nanoparticles [16, 17]. These structures manifest unique optical modes and dispersion relations in comparison with planar sheets, and can therefore be widely explored as promising building blocks for high-sensitive sensors [13], absorbers [18, 19], metamaterials [20, 21] and nano-waveguides [14, 22]. More importantly, the optical properties of graphene, including high field confinement and low dissipative loss, can be remarkably changed by controlling the charge density (Fermi energy) via chemical doping or electrostatic fields [23, 24]. Great attention has thus been triggered by these intriguing properties to investigate the light manipulation in graphene-based plasmonic systems [25, 26].

In the context of nonlinear optics, the significant merits by cooperating graphene in nanostructures comes from its ultra-large nonlinear coefficient verified by experiments [27], leading to enhanced nonlinear effects such as frequency conversions [17, 28] and optical switching [29]. Recently, graphene plasmonic solitons were predicted in planar sheets and ribbons [30–36], where various types of 1D solitons exist as counterparts to those in traditional dielectric/metal structures, with improved confinements. Temporal solitons in graphene-fiber lasers have also been widely reported [37].

In this paper, we propose a new type of periodic plasmonic nanostructure constituted by closely packed graphene-coated nanowires, in both 1D and 2D arrangements. With such configurations, we investigate the waveguides coupling, discrete diffraction, as well as nonlinear modes by strictly solving the Maxwell's equations. Our results demonstrate the existence of discrete solitons, whose characteristics, including the mode localization, the soliton power and the propagation length, exhibit feasible tunability through controlling the Fermi energy or the input beam intensity.

2. Theoretical model of graphene-coated nanowire arrays

We start by considering an array of nanowire waveguides periodically arranged along x direction, with an equivalent spacing of s between the neighboring nanowires, as depicted in Fig. 1(a). Each nanowire comprises a dielectric core with radius $a = 100$ nm and permittivity $\epsilon_c = 3.24$. A monolayer graphene, characterized by its complex conductivity σ , wraps the dielectric core tightly, and the whole array is then buried in a dielectric background of $\epsilon_b = 2.25$. The optical response of graphene, under a strong enough field, comprises a joint contribution of linear and nonlinear conductivity, $\sigma(\omega) = \sigma_L(\omega) + \sigma_{NL}(\omega)|E_t|^2$, where E_t is the tangential component of the electric field. In our simulated frequency range (mid-infrared spectrum), the linear term is primarily contributed by the intraband transition, which takes a Drude-like form within the random-phase approximation [5],

$$\sigma_L(\omega) = \frac{e^2 E_F}{\pi \hbar^2} \frac{i}{\omega + i\tau^{-1}}, \quad (1)$$

where E_F is the Fermi energy, ω is the angular frequency and $\tau \approx 0.5$ ps is the carrier relaxation time ($T = 300$ K) associated with plasmon decay in graphene. We neglect the interband transition in graphene because $E_F > \hbar\omega/2$ [5]. The nonlinear conductivity in the mid-infrared spectrum can be derived using a quasi-classic approach, written as [33, 38]

$$\sigma_{NL}(\omega) = -i \frac{3}{8} \frac{e^2}{\pi \hbar^2} \left(\frac{eV_F}{E_F \omega} \right)^2 \frac{E_F}{\omega}, \quad (2)$$

where $V_F \approx 10^6$ m/s is the Fermi velocity in graphene.

The graphene-coated nanowires could be fabricated via chemical-vapor-deposition (CVD) growth of high-quality monolayer graphene on the nanowire templates, where a flexible choice of core-diameter ranging from tens nanometers to several micrometers has been

demonstrated [39, 40]. Due to the van der Waals interaction, the graphene coating and the dielectric core are expected to be tightly attached together.

In our numerical model, we consider graphene as an ultra-thin film with a thickness of $t = 0.5 \text{ nm}$, of which the anisotropic bulk permittivity is characterized by $\epsilon_t = 2.5 + i\sigma / (\epsilon_0 \omega t)$ as the tangential element and $\epsilon_n = 2.5$ as the normal element [24]. Note that the intensity-dependent nonlinear conductivity only affects ϵ_t . The solving of electromagnetic field is performed within the framework of full-vector Maxwell's equations without approximation, using a finite element solver Comsol Multiphysics. Convergence tests are conducted to determine the appropriate sizes for the mesh and the computation window so that the accuracy of field distribution in the vicinity of graphene-nanowires can be guaranteed.

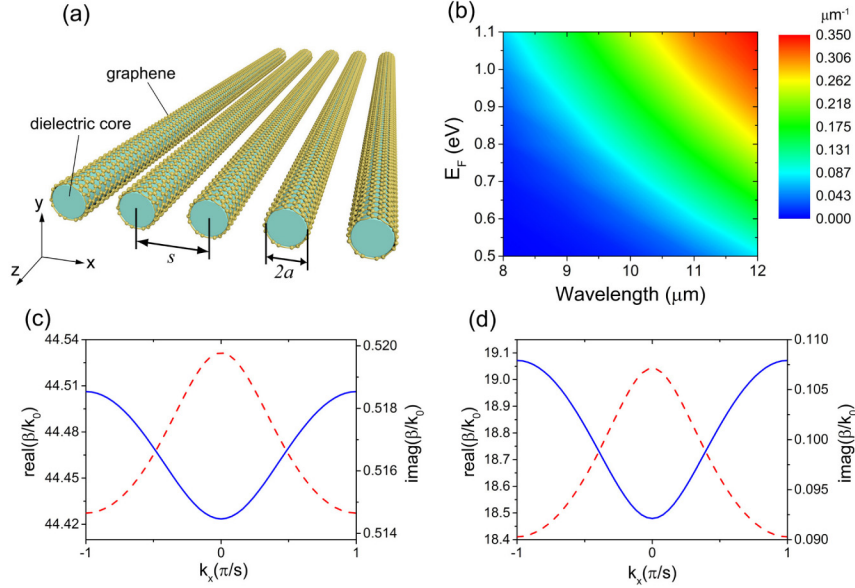


Fig. 1. (a) Schematics of an array of dielectric nanowires coated by graphene monolayer. (b) Influence of the wavelength and Fermi energy on the coupling coefficient for neighboring nanowires. (c), (d) Diffraction relation of the fundamental transmission band for (c) $E_F = 0.5 \text{ eV}$, (d) $E_F = 1.1 \text{ eV}$, with $\lambda_0 = 10 \mu\text{m}$. In (b)-(d), $a = 100 \text{ nm}$, $s = 4a$.

3. Band structures and soliton modes

3.1 One-dimensional arrays

Figure 1(b) plots the linear coupling coefficient of neighboring nanowires over a spectrum of free-space wavelength and Fermi energy, where the nonlinear contribution on conductivity is temporarily excluded ($\sigma_{NL} = 0$). The coupling coefficient is defined by $\kappa = |\beta_e - \beta_o|/2$, where β_e and β_o represents the real part of linear propagation constant of even and odd super-mode of two parallel nanowires. It can be seen that the waveguides show much smaller mutual coupling at short λ_0 and low E_F , due to the stronger field confinement for the isolated nanowire caused by the high mode-index in this regime. Notably, the coupling strength increases by 7.8×10^3 times from $4.5 \times 10^{-5} \mu\text{m}^{-1}$ ($\lambda_0 = 8 \mu\text{m}$, $E_F = 0.5 \text{ eV}$) to $0.35 \mu\text{m}^{-1}$ ($\lambda_0 = 12 \mu\text{m}$, $E_F = 1.1 \text{ eV}$), indicating a significant dispersion and tunability on the diffraction efficiency of SPP waves in the present lattice. In the following discussion, we fix the operation wavelength at $\lambda_0 = 10 \mu\text{m}$ and focus on the E_F related impacts. In Fig. 1(c) and 1(d), the linear diffraction relation of the 1D array is illustrated for various E_F . The

transmission band corresponds to the fundamental mode ($m=0$) that does not cutoff for small a and distributes evenly along the surface of the graphene coating. It can be seen that the real part of the diffraction curve minimizes at the Brillouin zone center ($k_x=0$), implying a negative coupling as in other types of plasmonic waveguides. The increased band curvature at $E_F=1.1\text{ eV}$ reflects the stronger discrete diffraction. Meanwhile, the imaginary part, which reflects the propagation loss of the Bloch modes, arrives at its minimum at the edge of the Brillouin zone ($k_x=\pi/s$), and significantly decreases as the coupling becomes stronger (at larger E_F).

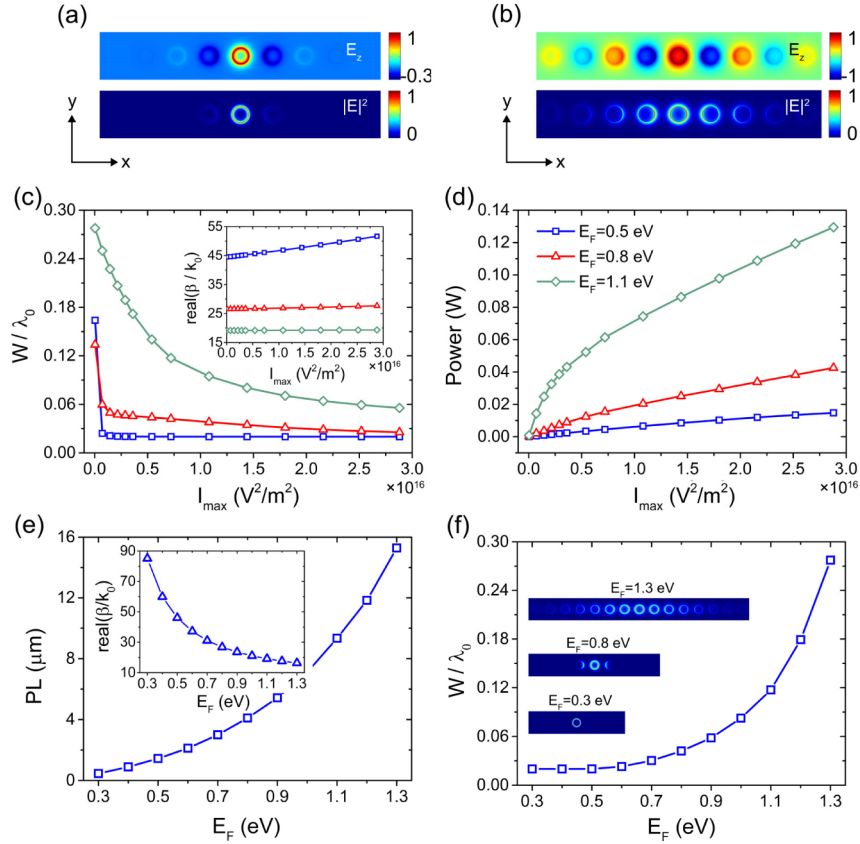


Fig. 2. Profiles of the normalized tangential electric field E_z and light intensity $|E|^2$ for 1D graphene-based solitons at different Fermi energy and beam intensity: (a) $E_F = 0.5\text{ eV}$, $I_{\max} = 3.6 \times 10^{14}\text{ V}^2/\text{m}^2$; (b) $E_F = 1.1\text{ eV}$, $I_{\max} = 7.2 \times 10^{15}\text{ V}^2/\text{m}^2$. (c) The normalized soliton width, [inset of (c)] soliton mode index and (d) soliton power vs. beam intensity. In (c) and (d), the blue, red and green curve represents $E_F = 0.5\text{ eV}$, $E_F = 0.8\text{ eV}$ and $E_F = 1.1\text{ eV}$, respectively. (e) The soliton propagation length, [inset of (e)] soliton mode index and (f) normalized soliton width vs. Fermi energy, for $I_{\max} = 7.2 \times 10^{15}\text{ V}^2/\text{m}^2$. The inset of (f) shows the $|E|^2$ soliton profiles at various E_F . In (a)-(f), $a = 100\text{ nm}$, $s = 4a$, $\lambda_0 = 10\text{ }\mu\text{m}$.

The generation of self-localized modes, i.e., discrete solitons, becomes possible when the nonlinear permittivity of graphene is taken into account ($\sigma_{NL} \neq 0$). Given the very low diffraction at certain Fermi levels and the giant nonlinear coefficient obtained from Eq. (2),

we expect highly confined solitons to exist with a moderate intensity. To explore this, we adopt a commonly used iteration scheme by updating the linear eigenmode solution consistently with a given intensity, until the stable nonlinear solution is obtained. Considering the self-focusing nonlinearity in graphene, the fundamental soliton supported by 1D arrays may only form at the Brillouin zone edge, which leads to a staggered phase pattern across the lattice period, as shown in Fig. 2(a) and 2(b). This is similar to the solitons found in graphene sheet arrays [31], but in contrast to the periodic modulated graphene monolayers [34], where the fundamental modes exhibit unstaggered patterns and dielectric-like band structures. It can also be observed that, compared with $E_F = 0.5\text{ eV}$, the enhancement of discrete diffraction at $E_F = 1.1\text{ eV}$ creates a much wider soliton profile along the x direction. To quantitatively analyze the localization degree of the solitons, we examine the dependence of soliton mode width

$$W = \left(\frac{2 \int |E|^2 (x-x_0)^2 dx}{\int |E|^2 dx} \right)^{1/2}, \quad (3)$$

with $x_0 = \int x |E|^2 dx / \int |E|^2 dx$ the mean center position, as a function of beam intensity I_{\max} [Fig. 2(c)]. The corresponding power is calculated using $P = (1/4) \iint_s [E \times H^* + E^* \times H] \cdot ds$. One can see that, when I_{\max} becomes larger, W decreases as the soliton propagation constant β penetrates into the semi-infinite band gap [inset of Fig. 2(c)]. Meanwhile, the power required for the deep-subwavelength confinement is found to be extremely low [Fig. 2(d)], For instance, when choosing $E_F = 1.1\text{ eV}$, a $0.1\lambda_0$ mode can be achieved by a power as small as 74 mW ($I_{\max} = 1.1 \times 10^{16}\text{ V}^2/\text{m}^2$). At a lower Fermi energy of $E_F = 0.5\text{ eV}$ (with the same I_{\max}), P reduces further to 7 mW while W approaches $0.021\lambda_0$, i.e., the whole soliton field has been tightly trapped close to the surface of the central nanowire. It is worth to emphasize that the generation of deep-wavelength ($10^{-2}\lambda_0$) plasmonic solitons is more realistic in the present configuration, as the required intensity is much lower than the damage threshold of graphene under femtosecond laser pulses ($\sim 10^{20}\text{ V}^2/\text{m}^2$) [41]. On the contrary, the miniaturization of conventional plasmonic solitons is primarily hampered by the stronger diffraction (due to the smaller mode index), which could request large nonlinearity unachievable by bulk materials.

Figure 2(e) depicts the dependence of the soliton propagation length, $PL = 1/[2\text{Im}(\beta)]$, on the Fermi energy, for $I_{\max} = 7.2 \times 10^{15}\text{ V}^2/\text{m}^2$. It shows that PL increases by 30 folds (from $0.5\ \mu\text{m}$ to $15.3\ \mu\text{m}$) as E_F varies from $0.3\ \text{eV}$ to $1.3\ \text{eV}$ (corresponding to a carrier density on the order of 10^{14} cm^{-2} [42]), while W changes from $0.02\lambda_0$ to $0.28\lambda_0$ [Fig. 2(f)]. On the other hand, the shift of light intensity has only weak influence on the PL . For example, corresponding to the increase of I_{\max} from $3.6 \times 10^{13}\text{ V}^2/\text{m}^2$ to $2.9 \times 10^{16}\text{ V}^2/\text{m}^2$ as in Fig. 2(c) and 2(d), the PL slightly changes from $1.5\ \mu\text{m}$ to $1.2\ \mu\text{m}$ for $E_F = 0.5\text{ eV}$; and changes from $9.6\ \mu\text{m}$ to $8.9\ \mu\text{m}$ for $E_F = 1.1\text{ eV}$. This result means that one can compress the soliton width by increasing I_{\max} without obviously increasing its dissipation. Therefore, by properly modulating the intensity of excitation beam and the Fermi energy of graphene coating, one has good flexibility to choose a desired compromise between the miniaturization and the propagation length of plasmonic solitons. Note that, in the lossy arrays, the self-action behavior can be significantly observed only if the soliton propagation length exceeds the coupling length. This condition is satisfied for $E_F \geq 1.1\text{ eV}$. To reduce loss and strengthen coupling, one can choose nanowires with larger radius, lower permittivity or operate at lower frequencies. It is also worth to mention that, the dissipation of graphene solitons is directly related to the value of relaxation time τ , thus a reduced propagation loss would be possible by using high-quality samples with enhanced mobility (thus longer τ) [43, 44]. Our simulation

shows that, for the highly compact 1D solitons at $\lambda_0 = 10 \mu\text{m}$, $E_F = 0.5 \text{ eV}$, the PL greatly raises from $0.3 \mu\text{m}$ to $14.4 \mu\text{m}$ as τ increases from 0.1 ps to 5 ps .

The performance of the present nanowire lattice solitons is similar to the reported discrete solitons in modulated monolayers [34]. For instance, with same conditions ($\lambda_0 = 10 \mu\text{m}$, $E_F = 0.5 \text{ eV}$, $I_{\text{max}} \approx 6 \times 10^{14} \text{ V}^2/\text{m}^2$), the soliton width ($\sim 0.03\lambda_0$) and mode power ($\sim 0.5 \text{ mW}$) are found to be comparable for both cases, although the larger size of nanowires (compared to the ultrathin graphene sheets) leads to a broader field distribution normal to the lattice periodicity (y direction). However, the nanowire structure provides the good possibility of constructing 2D arrays, in which the formation of 2D graphene solitons with complex field patterns are expected. We will explore this issue in the next section.

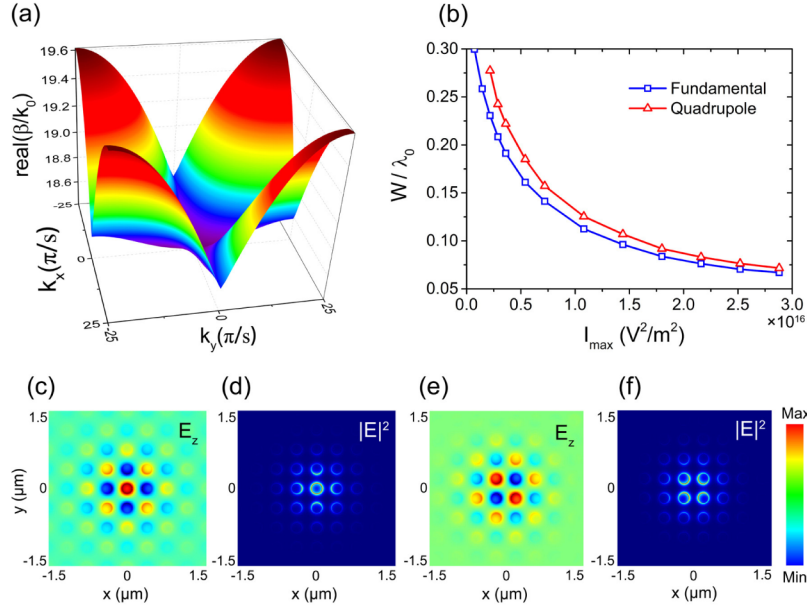


Fig. 3. (a) Diffraction relation of the fundamental transmission band for the 2D array, with $\lambda_0 = 10 \mu\text{m}$. (b) The normalized soliton width vs. beam intensity, for the fundamental and quadrupole modes. (c)-(f) E_z and $|E|^2$ profiles of the (c), (d) fundamental mode, and (e), (f) quadrupole mode, for $I_{\text{max}} = 2.2 \times 10^{16} \text{ V}^2/\text{m}^2$. In (a)-(f), $a = 100 \text{ nm}$, $s = 4a$, $E_F = 1.1 \text{ eV}$, $\lambda_0 = 10 \mu\text{m}$.

3.2 Two-dimensional arrays

Our present structure can be readily used to build 2D lattices by stacking 1D arrays along y axis in a square manner. In Fig. 3(a), the diffraction relation is sketched with $a = 100 \text{ nm}$ and $s = 4a$, $E_F = 1.1 \text{ eV}$. Similar to the 1D case, the negative coupling creates a concave surface in the vicinity of the Brillouin zone center and a convex at the edge of the fundamental band. Typical examples of the 2D solitons are illustrated in Fig. 3(b) and 3(c), showing the $|E|^2$ distribution of a fundamental ($W = 0.076\lambda_0$, $PL = 9.0 \mu\text{m}$) and a quadrupole ($W = 0.083\lambda_0$, $PL = 8.9 \mu\text{m}$) mode, respectively. We note that, although characterized by the four brightest spots, the quadrupole modes exhibit very similar width to that of the fundamental modes [Fig. 3(d)]. This can be understood by the stronger interaction between the brightest spots, which distorts the fields towards the central “gap” region, leading to an enhanced concentration for the quadrupoles.

Besides the fundamental band, we also find higher-order bands corresponding to the two degenerated $m=1$ nanowire modes (distinguished by a 90° rotation in their field distribution). The existence of multi-bands indicates that scalar or vector gap solitons could also be found in the proposed structures, with E_F controllable characteristics.

4. Conclusion

In conclusion, we have proposed a new type of plasmonic lattice built by 1D or 2D array of graphene-coated nanowires. The calculations have revealed the possibility of generating ultra-compact soliton modes with low power and acceptable dissipative loss. The strong tunability of discrete diffraction and mode properties may render the graphene-based solitons intriguing applications in nanoscale optical switching, signal processing and active nanophotonic devices.

Acknowledgments

This work has been supported by the Deutsche Forschungsgemeinschaft (DFG) via TRR142.